Sustainable Energy Technologies and Assessments 85 (2026) 104785

Contents lists available at ScienceDirect

Sustainable Energy Technologies and Assessments

journal homepage: www.elsevier.com/locate/seta

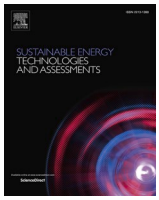

Original article

Ecotechnological Valorization of Verbesina encelioides: A dual strategy for sustainable biodiesel production and invasive weed mitigation

Farzana [a], Fahd A. Nasr [b], Mushtaq Ahmad [a,*], Mohammed Al-zharani [b], You-Cai Xiong [c], Lina M. Alneghery [b], Hong-Yan Tao [c], Najeeb Ullah [a], Ahmad Mustafa [d,*], Shazia Sultana [a]

[a] Bioenergy and Biodiversity Research Centre for Agro-biological Resources, Quaid-i-Azam University, Islamabad, Pakistan
[b] Biology Department, College of Science, Imam Mohammad Ibn Saud Islamic University (IMSIU), Riyadh 11623, Saudi Arabia
[c] State Key Laboratory of Herbage Improvement and Grassland Agro-ecosystems, College of Ecology, Lanzhou University, Lanzhou 730000 Gansu, China
[d] Center of Excellence, October University for modern Sciences and Arts (MSA), Giza, Egypt

ARTICLE INFO

Keywords:
Verbesina encelioides
Biodiesel
Co3O4 Nanocatalyst
Circular bioeconomy
Invasive Weed Management
Response Surface Methodology

ABSTRACT

The global shift towards renewable energy has intensified the need for sustainable technologies. The present study investigates the invasive weed *Verbesina encelioides* (Cav.) Benth. & Hook. Ex A. Gray as a potential feedstock for biodiesel production, while managing ecological issues. The seeds contain large amounts of oil (33 wt%) and a very low level of free fatty acids (0.16 wt%), which allows one-step transesterification using a synthesized cobalt oxide (Co3O4) nanocatalyst prepared from seed husk (a waste product) as a precursor. The nanocatalyst was characterized using Fourier-transform infrared spectroscopy (FTIR), scanning electron microscopy (SEM), energy-dispersive X-ray spectroscopy (EDX), dynamic light scattering (DLS), and X-ray diffraction (XRD). These techniques verified the porous morphology, cobalt-oxygen-rich composition, and highly crystalline structure, thereby confirming the presence of active catalytic sites. Response Surface Methodology (RSM) with a Box-Behnken Design (BBD) was used to optimize the reaction parameters. Such as oil methanol molar ratio of 1:3, catalyst loading of 0.4 % wt., reaction temperature of 60 °C, and reaction time of 120 min, confirming the conversion of triglycerides into fatty acid methyl esters (FAMEs) and yielding a maximum biodiesel production of 97 %. The resulting biodiesel was characterized by FTIR, 1H and 13C nuclear magnetic resonance (NMR), and gas chromatography-mass spectrometry (GC–MS), indicating complete transesterification, with oleic acid methyl ester as the dominant FAME. Compared to conventional diesel, the synthesized biodiesel exhibits high oxidative stability and standard combustion properties; the nanocatalyst also maintains recyclability and catalytic activity across multiple catalytic cycles. These results highlight the dual advantages of controlling an invasive species and generating high-quality biodiesel, which aids in designing bio-powered energy systems, efficient application technologies, and a circular bioeconomy.

Introduction

A sustainable energy approach is not only a reliability and viability concern, but it also sets the direction for low-carbon energy prospects [1]. Concurrently, the depletion of non-renewable energy resources is an important global issue. Given the rising demand for energy and an ever-increasing population, fossil fuels are expected to run out in the next 70 to 150 years [2]. Energy is a critical factor in economic development and a key to national development. Biofuel is a series of management strategies to reduce greenhouse gas emissions and limit global temperature rise [3]. Biofuel is a series of management strategies to reduce greenhouse gas emissions and limit global temperature rise [4]. Only 72 countries have adopted inclusive strategy frameworks to achieve net-zero carbon emissions technologies. The aggregate renewable energy capacity is projected to increase by 2.7 times in 2030. Moreover, the global average progress in 2024 is only 25, far below the target of 65, which requires an increase in action [5]. To address this situation, the use of alternative and synthetic fuels is increasingly being explored to

* Corresponding authors.
E-mail addresses: farzana@bs.qau.edu.pk (Farzana), faamohammed@imamu.edu.sa (F.A. Nasr), mushtaq@qau.edu.pk (M. Ahmad), mmyalzahrani@imamu.edu.sa (M. Al-zharani), xiongyc@lzu.edu.cn (Y.-C. Xiong), lmalneghery@imamu.edu.sa (L.M. Alneghery), beltroad@lzu.edu.cn (H.-Y. Tao), Najeebullah@bs.qau.edu.pk (N. Ullah), ammhamed@msa.edu.eg (A. Mustafa), shaziaflora@hotmail.com (S. Sultana).

https://doi.org/10.1016/j.seta.2025.104785
Received 2 September 2025; Received in revised form 26 November 2025; Accepted 13 December 2025
Available online 3 January 2026

reduce dependence on fossil fuels and non-renewable energy sources [6]. The overall energy implications show a shift toward balancing renewable energy sources, especially biomass. Biodiesel from renewable sources appears to be a good alternative to improve energy security [7]. Biofuels provide a net energy gain, are eco-friendly and cost- effective, and do not compete with food resources [8]. Production of biodiesel from various feedstocks is expected to reach around 36 billion liters worldwide, with Europe, particularly Germany, at the forefront of both production and consumption [9].

Biodiesel is produced by the transesterification of triglycerides derived from oils such as vegetable oils, animal fats, microbial oils, algae, and waste oils. The process uses monohydric alcohols, primarily methanol or ethanol, to produce fatty acid alkyl esters, primarily fatty acid methyl esters (FAMEs) [10]. This methodology is preferred due to the high product yield and economic feasibility [11]. Catalysts are crucial for improving reaction rate, final yield, and biodiesel quality [12]. In the current study, a phosphorus nanocatalyst was produced by mixing cobalt chloride with the waste product, seed husk, for efficient biodiesel production. The nanocatalyst has an increased surface area, which increases reaction rate, enhances product yield, and reduces by-product formation, due to its enhanced catalytic activity [13]. The effectiveness of the metal oxide-based catalyst among several feedstocks, including the third-generation non-edible feedstock, has been demonstrated [14]. Additionally, the use of phytogenic materials promotes the sustainability of the catalyst by reducing environmental impact [15].

We explored the dual nature of cobalt oxide as a nanoparticle and a heterogeneous catalyst and tested its activity over several reaction cycles [16]. The catalyst's recyclability highlights its sustainability, as it can be recycled without significant loss of activity over multiple cycles [17]. As a result, a recyclable phyto-nanocatalyst is a potential alternative for sustainable biodiesel production, though the use of edible oils has raised serious issues concerning food security, leading to food vs. fuel conflict, particularly in developing countries where hunger and economic security are major challenges. These emphasize the search for alternative sources for biodiesel production. The use of non-edible oils for biodiesel production is a sustainable approach that does not cause food shortages [18]. In particular, invasive plant species that exhibit excessive growth and contain high oil content have also been reported as possible feedstocks for the synthesis of biodiesel [19].

A wide range of studies has been conducted on the production of biodiesel from edible and non-edible oils, as shown in Table S1. However, our study introduces a novel approach by using the non-edible oil from an invasive weed, thereby contributing to the control of the invasive species and reducing ecological harm. To improve the energy resource issue, Verbesina encelioides seed oil was investigated for the first time as a potential feedstock for biodiesel by measuring its oil yield and free fatty acid (FFA) content, along with the novel synthesis of cobalt oxide phyto-derived nanocatalyst using the seed husk of *V. encelioides and* cobalt chloride salt. Response Surface Methodology (RSM), a numerical modeling technique, was used to determine optimal conditions to improve reaction efficiency and product quality. Advanced analytical techniques were applied to study the crystalline structures and functional groups of the synthesized cobalt oxide, including Fourier Transform Infrared Spectroscopy (FTIR), Dynamic Light Scattering (DLS), Scanning Electron Microscopy (SEM), Energy Dispersive X-ray Spectroscopy (EDX), and X-ray Diffraction (XRD). The synthesized biodiesel was quantitatively identified using FTIR, Gas Chromatography-Mass Spectrometry (GC–MS), and Nuclear Magnetic Resonance Spectroscopy, both 1H and 13C NMR. FTIR analysis of seed oil identified its chemical composition and functional groups, enabling evaluation of its bioactive potential.

Materials and methods

Various non-agronomic plants produce unusual triacylglycerols in their seed oils, which exhibit distinct properties, making them advantageous for various industries [20]. *Verbesina encelioides* (Cav.) Benth. & Hook. Ex A. Gray shown in plate.S1 is a sustainable feedstock for biodiesel production bearing numerous seeds as each flower produces 300–350, and an individual plant generates 600–2,100 seeds with high oil content up to 31 % [21,22]. The Seeds were collected from the northern area of Pakistan, along the roadsides of the Malakand Pass Hills, which lie at 35.2130°N and 71.8700°E, and were manually separated from the flower tops. Dried in the shade and stored in clean airtight glass jars to prevent contamination.

Oil content determination

Soxhlet extraction is a common method for determining oil content [23]. A 5-gram powdered sample was placed in a thimble and extracted with an ethanol-n-hexane solvent mixture (1:2, respectively). This extraction procedure, which involved heating the solvent mixture in a water bath, was repeated several times by recycling the solvent through condensation. The methanol was then evaporated using a rotary evaporator, and the extracted oil was measured to determine the final yield [24]. The Thimble computation was performed using the following equation 0.1 [25].

$$\text{Oil content yield (wt. \%)} = \frac{A - B(C - B)}{D} \times 100 \quad (1)$$

Computations using round bottom flask were obtained by applying the following equation.2. [26]

$$\text{Oil content yield (wt. \%)} = \frac{A - B}{D} \times 100 \quad (2)$$

As,

A = thimble weight + powdered sample weight.

B = empty thimble/flask weight.

C = empty thimble/flask weight + powdered sample weight after extraction.

D = sample weight.

Oil extraction

Mechanical oil extraction is preferred, eliminating the need for chemical solvents and enhancing safety and stability. To facilitate the filtration process, the crude oil was heated and then filtered through porcelain filter paper to remove impurities, thereby improving the yield of biodiesel. The filtered oil was then collected in a flask and measured in a graduated cylinder [27]. To preserve the chemical quality and prevent light-induced oxidation, the oil was stored in dark color glass bottles. To maintain the chemical integrity and minimize photooxidation, the oil was kept in amber glass bottles. The percentage yield of the seed oil was calculated using Equation 3 [28].

Oil content yield (wt%) $= \frac{A-B(C-B)}{D} \times 100$ (3).

Free fatty acid content determination

The quality and stability of oils and fats are checked by measuring their FFA content. A titration-based technique, the AOCS method CD 3d-63, provided precise results by determining FFA as the volume of alkali required to neutralize free acids in the oil [29]. For measuring FFA content, 1 mL of oil was mixed with 9 mL of isopropanol and a few drops of phenolphthalein indicator.

While stirring, the oil solution was titrated with 0.14 N potassium hydroxide (KOH) until a stable pink color persisted for 30 s, marking the endpoint. To ensure accuracy, the titration was repeated three times. The free fatty acid content of crude oil is calculated using an equation.4

$$Acidvalue = \frac{v_2 - v_1}{vt} \times wt \quad (4)$$

As,

v2 = Volume of KOH solution utilized for sample volumetric analysis.

v1 = Volume of KOH solution utilized for blank volumetric analysis.

wt = Weight of KOH in mg per liter.

VT = total amount of crude oil.

Synthesis of phyto-derived cobalt chloride nano-catalyst from V. encelioides seed husk

Utilizing agricultural waste for nanocatalyst synthesis is an innovative and sustainable approach. Plant-derived resources offer potential biocompatibility and an eco-friendly nature, which are beneficial for catalyst synthesis. The phyto-nanocatalyst synthesized from cobalt chloride in association with an aqueous plant extract adheres to the principles of green chemistry by employing a sustainable methodology [30]. In-situ impregnation was used for the fabrication of the phyto-nanocatalyst using the seed husk of V. encelioides, as shown in Fig. S2. To improve the catalytic potential and the surface characteristics, a series of pretreatments of seed husks was performed [31]. Before grinding, the husks were washed with distilled water to remove impurities and then dried in an oven at 25℃ for 30 days. Fifty grams of milled husk material was then boiled in 500 mL of distilled water at 350 degrees centigrade on the hot plate for 4 h, with constant stirring, to give a thick, gelatinous extract. The extract was filtered to obtain a clear solution of 50 mL. A 0.2 M solution of cobalt chloride ($CoCl_2{\cdot}6H_2O$) was prepared by dissolving 0.2 g of $CoCl_2{\cdot}6H_2O$ in 30 mL of distilled water, then heating at 60 °C for 30 min with continuous stirring. The aqueous extract is then added to the salt solution. Phytochemicals in the aqueous plant extract act as reducing agents, transforming cobalt ions into nanoparticles. To facilitate the crystallization and structural transformation of cobalt compounds, the mixture is heated to 70 °C for two hours and kept in the oven at 65–100 °C for 2–3 days. For critical catalytic activity, calcination was performed at 500 °C for 2 h to promote the formation of cobalt oxides and oxychlorides [32]. The catalytic activity is further assessed by their efficiency in converting oil to biodiesel via transesterification [33].

Characterization of the synthesized catalysts, biodiesel, and seed oil from V. encelioides

Various techniques were employed to characterize the synthesized phyto-nanocatalyst, seed oil, and biodiesel derived from *V. encelioides*. To identify the functional groups and chemical bonds, FTIR spectroscopy using the Bruker Alpha II model with a scanning range of 500 to 4000 cm^{-1}. For detailed crystallographic analysis, the catalyst was examined by powder X-ray diffraction (XRD) using a Bruker D8 diffractometer with Cu-Kα radiation (λ = 1.54 Å) and a 2θ range of 10° to 60° at 2°/min.

Dynamic light scattering (DLS) measurements were performed using a Malvern Panalytical Zetasizer (UK) to assess the surface charge and colloidal stability of the nanocatalyst. The surface morphology and structural features of the catalyst were examined with the scanning electron microscope (SEM) with an operating voltage of 30 kV on the JEOL JSM-5910 SEM. Elementary composition was determined using Energy − Dispersive X - Ray Spectroscopy on an INCA-200 system from Oxford Instruments (UK). Recent studies have shown that, together, these analytical techniques provide an overall understanding of the physical, chemical, and structural features needed for the sustainable use of the catalyst [34]. Fourier Transform Infrared (FTIR) spectroscopy was used to detect functional groups in the synthesized biodiesel and seed oil, particularly the ester carbonyl, to confirm the success of the transesterification process. The Bruker Alpha II spectrometer was used for these measurements. The molecular composition and the structural properties of the synthesized biodiesel were further elucidated using Nuclear Magnetic Resonance (NMR) spectroscopy. Both^1H NMR and^13C NMR spectra were recorded at 300 MHz and 20 °C using deuterated chloroform (CDCl3) as solvent on a Bruker NMR system using a 5 mm PROBHD BBO BB-1H probe. The elemental profile of biodiesel was also studied by Gas Chromatography-Mass Spectrometry (GC–MS) on an Agilent Technologies 7890B GC system and 5977 Mass Spectrometer (MS), USA [35].

Synthesis of biodiesel using phyto-nano catalyst

Non-edible seeds with High oil content and low FFA values are potential feedstock for biodiesel production. For oils with low FFA content, a single transesterification step is done. For the transesterification reaction, Methanol was used as the alcohol, considering the noted quantities of each variable, i.e., the catalyst loading, reaction temperature, reaction time, and oil-to- methanol ratio from the experimental design Table S5. After completing the methoxide reaction at 60 °C for 40 min, 10 mL of preheated oil was added to the mixture. The methanol was removed from the biodiesel using a rotary evaporator. The Glycerol and catalyst residue were separated after transesterification was complete. Equation 5 was used to calculate the biodiesel yield. To optimize the yield of biodiesel, the transesterification reaction was tested 5 times, with reaction parameters adjusted accordingly, as shown in Table S5. [36,37].

$$\text{Yield of biodiesel} = \frac{weightofbiodieselingrams}{weightofoil} \times 100 \quad (5)$$

Experimental design

To improve biodiesel yield, 30 experiments were conducted with four variables (A–D). i.e., oil to methanol ratios (1:6–1:18), catalyst concentration (0.4–0.12 wt%), temperature (60—100 °C), and reaction durations (60–120 min) [38]. The optimization was performed using Response Surface Methodology (RSM) with a Box-Behnken Design (BBD) in Design-Expert 13 (Stat-Ease Inc., Minneapolis, USA). Factor interdependence was analyzed using a quadratic response surface model, while ANOVA was employed to validate the model and optimize reaction conditions. Table 1.

Reusability of catalyst

The high reusability of the cobalt oxide nanocatalyst was evaluated to verify its activity retention over multiple cycles of biodiesel synthesis via transesterification. In accordance with the methodology of [39] with some subsequent modifications, the catalyst was recovered after each reaction cycle by filtration. It was then washed thoroughly with distilled water to remove the remaining reactants and by-products and then dried in an oven at 65℃ for 3 h to achieve complete moisture removal. The robustness of the catalyst under different conditions was investigated by measuring catalytic effectiveness over 5 successive transesterification cycles under varying reaction conditions, including temperature, catalyst amount, and methanol- to-oil molar ratio.

Results and discussion

Oil and FFA composition of Verbesina encelioides

Species with higher FFA levels, such as *Xanthium strumarium* (28–31 wt% oil, 2–4 wt% FFA) and *Artemisia annua* (18–26 wt% oil, 3–5 wt% FFA), require a two-step transesterification process. *V. encelioides* is an exceptional biodiesel feedstock within the *Asteraceae* species based on high oil yield (33 wt%) and low FFA (0.16 wt%) values, making single-step transesterification a cost-effective process. However, *Helianthus annuus* (20–28 wt% oil, 0.5–2 wt% FFA) and *Carthamus tinctorius* (20–36 wt% oil, 1–2 wt% FFA) require further processing. *Tagetes*

Table 1
ANOVA for the Response Surface Quadratic Model for *V. encelioides.*

Source	Squared total	df	Quadratic mean	f-statistic	p- statistic	
Model	2396.04	14	171.15	4.04	0.0055	significant
A-Oil to Menthol Ratio	5.51	1	5.51	0.1301	0.7233	
B-Catalyst Conc.	208.27	1	208.27	4.92	0.0424	
C-Temp	124.67	1	124.67	2.94	0.1068	
D-Time	40.82	1	40.82	0.9640	0.3417	
AB	346.89	1	346.89	8.19	0.0119	
AC	117.18	1	117.18	2.77	0.1169	
AD	356.27	1	356.27	8.41	0.0110	
BC	300.16	1	300.16	7.09	0.0177	
BD	310.64	1	310.64	7.34	0.0162	
CD	3.33	1	3.33	0.0787	0.7830	
A^2	440.46	1	440.46	10.40	0.0057	
B^2	5.13	1	5.13	0.1211	0.7327	
C^2	5.08	1	5.08	0.1199	0.7340	
D^2	162.27	1	162.27	3.83	0.0691	
Residual	635.15	15	42.34			
Lack of Fit	324.08	10	32.41	0.5209	0.8222	not significant
Pure Error	311.07	5	62.21			
Cor Total	3031.18	29				

minuta, which requires pre-treatment and has 16–22 wt% oil and 1.5–3 wt% FFA, needs further pre-treatment that agrees with biodiesel optimum values [40].

In addition to its oil yield, *V. encelioides* biodiesel properties, including a high proportion of unsaturated FAMEs, oleic and linoleic acids, improve cold flow properties and oxidative stability, similar to those of *Helianthus annuus* and *Carthamus tinctorius* [41]. However, *V. encelioides has* a favorable saturated-to-unsaturated FAME ratio, which is conducive to enhanced combustion efficiency, a higher cetane number, and increased energy density. Non-edible species of *Asteraceae* which can be used as potential feedstock include *Tithonia diversifolia* (18–30 wt% oil, 1.5–4 wt% FFA), *X. strumarium* (25–28 wt% oil), and other members of the genus *Xanthium* with the oil content of 1–40 wt% and FFA content ranging from 6.7–58 wt%.

Characterization of phyto-derived cobalt oxide nano catalyst

a) *FTIR of cobalt oxide nano catalyst*

The FTIR spectrum of the nano catalyst exhibited a broad peak at 3100–3500 cm^{-1}, indicating O–H stretching from absorbed water or hydroxyl groups, while a sharp peak at ~ 1600 cm^{-1} corresponded to bending vibrations of water molecules Co-Cl stretching absorptions in the 500–1000 cm^{-1} range confirm cobalt-chloride coordination; peaks in the 1400–1500 cm^{-1} range signify the existence of carbonyl groups as shown in Figure.1 [42], Identified the 3100–3500 cm^{-1} peaks in Co-based nano- catalysts as indicative of surface-bound hydroxyl groups crucial for catalytic activity in water–gas shift and electrochemical reactions. Similarly, [43] assigned the ~ 1600 cm^{-1} peak to water molecules adsorbed to the surface, important for CO_2 reduction and hydrogen evolution. The 500–1000 cm^{-1} absorptions in cobalt-based electrocatalysts were linked by [44] to Co– Cl stretching, which stabilizes active sites and enhances electron transfer. According to [45], the 1400–1500 cm^{-1} peaks are attributed to residual carbonyl groups, which enhance conductivity and charge transport in nano-catalysts. The spectral sequence proved the existence of active sites in the nano-catalyst, including hydroxyl and carbonyl groups, and Co-Cl

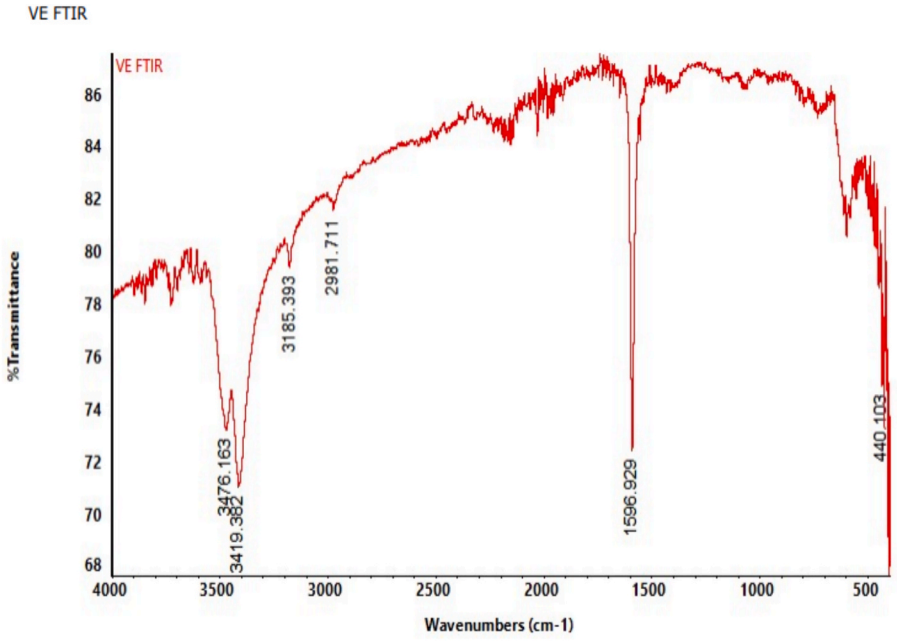

Fig. 1. FTIR spectrum of Cobalt oxide Nano catalyst.

coordination, which is an indicator of increased efficiency and stability in the principle of CO2 reduction and hydrogen production.

b) *DLS analysis of cobalt oxide nano catalyst*

Fig. S3. The present Dynamic Light Scattering (DLS) of the nano-catalyst revealed that cobalt oxide nanocatalysts are aggregated, with a Z-average size of 14,336 nm, a PDI of 0.449, and a primary peak of 97.76 nm. The D10, D50, and D90 values are 72.57 nm, 88.49 nm, and 113.03 nm. In Table S2. The size distribution of Cobalt oxide nano catalyst size between 72.57 nm (D10) and 12,823 nm (100). The summary parameters of the Cobalt oxide nanocatalyst indicate a narrow size distribution, stability, and catalytic activity, as reported in Table S3. These values are consistent with earlier findings, which indicated that the size distribution of cobalt oxide nanoparticles ranged from 50 to 150 nm [46].

c) *SEM of cobalt oxide nano catalyst*

The evaluation of cobalt chloride nano-catalysts by scanning electron microscopy (SEM) is shown in the Plate. S3 presents nano-scale topographic profiles, including porosity and agglomeration. The strong surface area and porosity at 2500x indicate many active sites, and the crystalline arrangements visible at 5000x suggest a high reactivity. These findings are supported by prior studies demonstrating that nanoscale characteristics and high porosity enhance the reaction rates of hydrogen evolution reactions (HER) and oxygen reduction reactions (ORR). According to results [47], cobalt oxide catalysts in agglomerated form exhibit greater stability and higher electrical conductivity [48] highlights the importance of hollow morphologies in facilitating the diffusion of reactants and the desorption of products, both crucial to water splitting and CO2 reduction. Nano-catalysts of cobalt chloride based on natural precursors, therefore, provide an attractive opportunity for sustainable energy storage and conversion technologies.

d) *The EDX spectrum of nano catalyst*

Table S4. Reports the EDX spectrum Fig. 2. By giving elemental composition and equivalent energy levels (keV). The data show that cobalt (46.86) is the major constituent of the cobalt-oxide nanocatalyst, and oxygen (42.48 3) indicates the presence of oxide species. Chlorine (7.72 %) is identified at 6.7 keV, and small traces of potassium and calcium are also identified. These findings are in agreement with those in reference [49], which highlighted cobalt-oxygen interactions in catalytic activity, and reference [50], which reported that chlorine can stabilize cobalt chlorides. In line with this, the results support the potential application of the cobalt chloride nanocatalyst in energy and environmental contexts.

e) *XRD of cobalt oxide nano catalyst*

X-ray diffraction (XRD) is a widely used analytical method for characterizing the crystalline structure, phase composition, and average crystallite size of nanomaterials. The XRD pattern of the synthesized cobalt oxide nanocatalyst, shown in Fig. 3, exhibits well-defined diffraction peaks confirming its crystalline nature. The diffractogram spans 10°-80° and has relative intensities between approximately 60 and 280 arbitrary units (a.u.). The strongest diffraction peaks are observed at approximately 19° and 37° 2θ, corresponding to the lattice planes 200 and 202, respectively. These observations are characteristic of the spinel phase of Co3O4, thereby validating the formation of a phase-pure, crystalline cobalt oxide structure. The high-intensity profile at 19° 2θ for the (200) plane indicates a dominant orientation, supporting the successful synthesis of the nanoparticles and their lower amorphous content. The fact that the (202) plane appears simultaneously at 37 degrees, whether it was at 37 degrees, is yet another trait that supports the comprehensive crystalline structure, which is likely to increase the surface area and consequently boost the catalyst's activity. Small variations in the background intensity may be attributed to the presence of organic species or incomplete decomposition of plant-based precursors used in the synthesis process [51]. The XRD pattern generally supports the high purity and structural integrity of the cobalt oxide nanocatalyst. The crystallite size (D) was calculated through the Scherrer equation. [48]

$$D = \frac{K\lambda}{\beta COS\Theta}$$

where:

D = average crystallite volume (nm).
K = shape factor (typically 0.9).
λ = X-ray wavelength for Cu Kα (0.154 nm).
β = Full Width at Half Maximum (FWHM) in radians.
Θ = Bragg angle (in radians).

Using the peak at 19° (200plane) and an estimated FWHM of 0.85°, the crystallite size of the cobalt oxide nanoparticles was found to be approximately 11.2 nm. This nano-scale dimension is ideal for catalytic applications, as smaller particle sizes provide a higher surface-to-volume ratio and greater density of active sites [52]. These structural features make the cobalt oxide nanocatalyst highly suitable for applications in energy storage, environmental remediation, and biodiesel production.

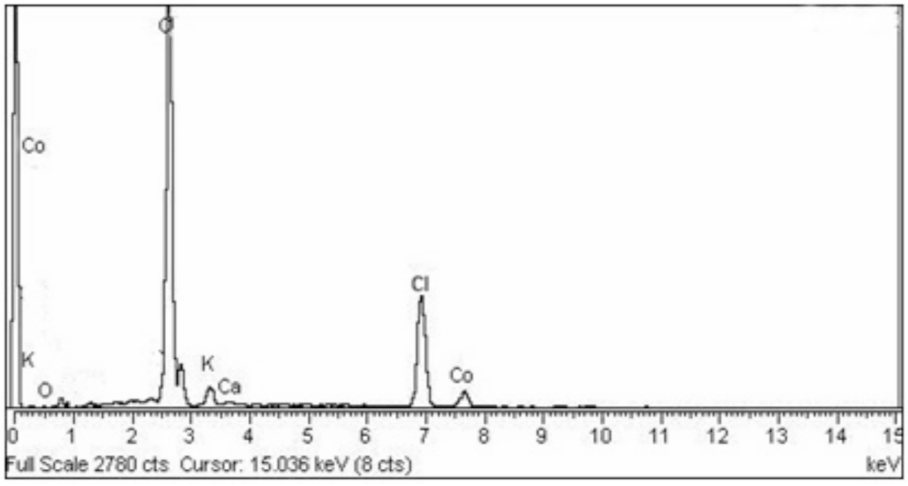

Fig. 2. Elemental compositions of Cobalt oxide catalyst through EDX.

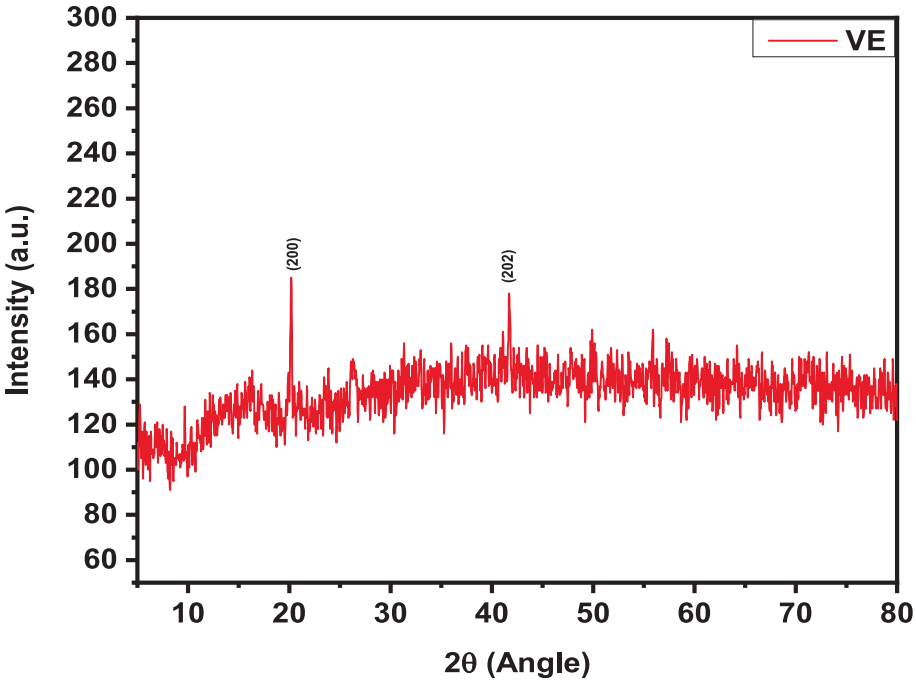

Fig. 3. XRD image of Cobalt Oxide Nano catalyst.

Cobalt oxide

Phyto-nano catalyst successfully converted *V. encelioides* seed oil into biodiesel with a high yield of 97 % through single-step transesterification. The optimal operating conditions were determined to be an oil-to-methanol molar ratio of 1:3, a catalyst loading of 0.4 wt%, a reaction temperature of 60 ℃, and a reaction time of 120 min, as indicated in Table S5. These results align with the literature findings discussed by [53], which demonstrate that metal-oxide catalysts enhance the efficiency of biodiesel production.

Properties of the fuel of Verbesina encelioides biodiesel

The fuel properties of *V. encelioides* biodiesel are presented in Table S6. showing excellent compliance with international standards (ASTM D6751 and EN 14214). The measured density (875 kg/m^3) falls within the acceptable range specified by the standards, ensuring efficient atomization and smooth engine performance. The kinematic viscosity at 40℃ (4.1 mm^2/s) is also well within the limitations and provides excellent flow characteristics and lubrication, supporting good combustion. The flash point (165 ℃) is considerably higher than the required minimum value, indicating high thermal stability and safety during handling and storage, as well as the absence of residual alcohols. Moreover, the acid value (0.40 mg KOH g-1) is below the allowed limit, confirming good chemical stability, proper conversion efficiency, and minimal degradation. Overall, these results confirm that *V. encelioides* biodiesel has excellent fuel quality, safety, and stability, making it suitable for use in diesel engines.

Statistical significance and validation of RSM model

The quadratic response surface model applied to *V. encelioides* (Table 1) demonstrated good statistical validity, as indicated by a significant F-value of 4.04 and a corresponding p-value of 0.0055, thereby confirming the adequacy of the model. Catalyst concentration (B) was found to be a statistically significant parameter influencing the biodiesel production ($p = 0.0424$). On the other hand, oil-to-methanol ratio (A), temperature (C) and reaction time (D) were not individually significant ($p > 0.05$) but the presence of several interaction terms (AB, AD, BC, BD) and the quadratic term (A2) showed significant effects ($p < 0.05$) implying strong synergistic and nonlinear interdependencies among the variables. The non-significance ($p = 0.8222$) of the lack-of-fit test confirmed the good agreement of experimental observations with model predictions. The coefficient of determination ($R2 = 0.7905$) and the adjusted R2 (0.6207) of the model further indicate the model's high predictive precision, which explains around 79 % of the variation in biodiesel yield. Consequently, the RSM model exhibits good statistical robustness and predictive reliability in optimization of biodiesel production from *V. encelioides* oil. Even though the oil-to- methanol ratio (A), temperature (C), and reaction time (D) were not significantly different as independent variables (p-value > 0.05), there were significant interaction values, such as the oil-to-methanol ratio and reaction time (AD), with an F-value of 8.41 There were also nonlinear effects related to the square of reaction time (D^2), which further supported the findings of [54]. The non-significant p-value of the adjusted lack-of-fit test ($p = 0.8222$) confirmed the model's reliability, as proposed by [55].

Interaction effects

1. Effect of methanol-to-oil ratio (A: MR) and catalyst concentration (B: CC%)

The 3D surface in plate S2. Shows a distinct curve, signifying a strong interaction between the methanol-to-oil ratio and catalyst concentration. There is a large increase in yield, reaching a maximum before declining thereafter, which is typical of an optimal region.

Effect of Catalyst Concentration (B): At a low methanol-to-oil ratio, the effect of increasing catalyst concentration is comparatively low, which was previously discussed by [56] In contrast, at intermediate and high methanol ratios, increases in catalyst concentration lead to a large increase in product yield, culminating in a maximum of around 90 % yield, as confirmed by [57] Beyond this optimum concentration, additional increases in catalyst dosage led to decreasing yields. This attenuation is typical for the system and can be attributed to high viscosity and the growth of side reactions, such as saponification, which consumes catalyst and consequently decreases the yield of biodiesel.

Effect of Methanol to Oil Ratio (A): Accordingly, for a fixed catalyst concentration, increasing the methanol to oil ratio increases the yield up to a certain limit, after which, excess methanol can dilute the reaction medium or complicate the separation of glycerol to give a decreased overall yield.

2. Effect of methanol to oil ratio (A: MR) & reaction temperature (C: Temp)

The three-dimensional surface shown in plate S2 exhibits a strong saddle-like or ridge morphology, which is a complex function of the methanol-to-oil ratio and temperature. This morphology contradicts a simple domelike topology, suggesting that the optimal methanol ratio is strongly temperature dependent.

Effect of Reaction Temperature (°C): Temperature has a significant effect on product yield. For lower values of the methanol- to-oil ratio, an increase in temperature has a very beneficial effect on the yield, as reported by [58]. The highest yields, near 97 %, are obtained at the highest temperature setting, due to faster reaction kinetics, resulting in a shorter time to reach equilibrium.

Effect of Methanol to Oil Ratio (A): The effect of the methanol to oil ratio is highly modulated by the temperature. At higher temperatures, a broader range of methanol ratios can achieve high yields, whereas at lower temperatures the optimal range is much narrower. As a result, a dominant determinant is the reaction temperature. Attainment of yields >=97 % requires a high reaction temperature; at this temperature, the methanol ratio can be fine-tuned within a moderate range to achieve the yield optimum.

3. Effect of methanol-to-oil ratio (A: MR) and reaction time (D: Time)

The 3D plot surface is shown in plate S2. shows a gradually rising ridge, indicating that the yield increases concomitantly with both the methanol-to-oil ratio and reaction time, until a maximum is reached, corresponding to the maximum yield.

Effect of Reaction Time (D): From a theoretical perspective, longer reaction times initially result in a marked improvement in product yield because the transesterification reaction has more time to proceed towards completion. The plot shows how, beyond a certain time, the incremental gains flatten off and the yield levels off at its maximum, around 97 percent.

Effect of Methanol-to-Oil Ratio (A): As with the time dependency trend, an optimum point is observed in the methanol-to-oil ratio. The highest yield plateau is reached at an intermediate ratio, provided the reaction time is long enough. While it is important to have sufficient reaction time for high conversion, excessively long times do not necessarily yield significant improvements and may reduce economic viability. Therefore, judicious selection of the methanol ratio and reaction time is very important for optimal performance. These observations agree with the results presented in references [59,60].

4. Effect of catalyst concentration (B: CC %) and reaction temperature (C: Temp)

The 3D plot surface in plate S2. Forms a gently curved surface with a clear peak region, showing that catalyst concentration and temperature have a meaningful interaction. The highest biodiesel yields (approaching 97 %) occur when the temperature is moderately high, and the catalyst concentration is in the mid-range. Both very low and very high catalyst concentrations reduce the yield.

Effect of Catalyst Concentration (B): At lower temperatures, increases in catalyst concentration improve the yield only moderately. At higher temperatures, the yield rises more sharply with catalyst concentration until it reaches an optimum, after which the yield declines. The decline at high catalyst concentration again suggests undesirable effects such as increased mixture viscosity or side reactions (e.g., soap formation), which interfere with the transesterification process as previously discussed in studies by [61]. Effect of Reaction Temperature (°C): shows a strong positive effect on yield. Increasing temperatures significantly improve product yield, especially when combined with the optimal catalyst concentration. However, temperature alone cannot compensate for an excessive catalyst concentration, as the downward slope beyond the optimum remains noticeable. The maximum biodiesel yield is achieved by a balanced combination of moderate catalyst concentration and elevated reaction temperature. Both insufficient and excessive catalyst levels reduce yield, especially at lower temperatures.

5. Effect of catalyst concentration (B: CC %) and reaction time (D: Time)

The BD plot shows a rising, then slightly declining, dome-shaped surface. Reaction time and catalyst concentration interact positively up to their optimal region. As both factors increase, the yield increases significantly until the plateau or peak region is reached.

Effect of Reaction Time (D): The yield increases steadily with reaction time, especially when the catalyst concentration is within the optimal range. Beyond a certain reaction time, further increase produces minimal improvement, indicating that equilibrium has been reached. Extremely long reaction times are therefore not economically beneficial.

Effect of Catalyst Concentration (B): initially, increasing the catalyst concentration boosts the yield by accelerating the transesterification reaction.as shown in the 3D surface plate S2. A similar inference is reported by [62,63]. However, at higher catalyst loadings, the yield drops due to issues such as soap formation and hindered phase separation. The effect is more pronounced when the reaction times are reduced. A properly selected catalyst concentration combined with adequate reaction time produces high biodiesel yields. Excess catalyst cannot replace insufficient reaction time, nor can a long reaction time compensate for excess catalyst.

6. Effect of reaction temperature (°C: Temp) and reaction time (D: Time)

This 3D plot displays a strong upward-sloping surface with a broad plateau at the top, indicating that both temperature and time strongly and positively influence yield until equilibrium conditions are reached.

Effect of Reaction Temperature (°C): has a dominant and highly positive effect on biodiesel yield. As the temperature increases, the reaction rate increases, allowing the system to reach high conversion quickly. At high temperatures, even moderate reaction times produce yields close to the maximum (~97 %).

Effect of Reaction Time (D): Longer reaction times steadily increase yield until reaching a plateau. At high temperatures, shorter times are required to reach the plateau, demonstrating the strong kinetic advantage of elevated temperature. As suggested by [64], the 3D surface plate. S2 shows that at lower temperatures, much longer times are required to achieve the same level of conversion. Temperature and reaction time show a synergistic relationship: higher temperatures accelerate the attainment of equilibrium by reducing the required reaction time. Attaining near-maximum yields requires having high temperatures while maintaining sufficient reaction time.

Model validation and diagnostic analysis

The diagnostic Predicted versus Actual plot in Fig. S9. validates the high accuracy of the developed response surface methodology (RSM) model, as seen, since the data points are close to the line of perfect agreement. This robust correlation, with a high coefficient of determination (R2) and low error measures, demonstrates good agreement between predicted and experimental biodiesel yields, ranging from about 50 % to 97 %. The uniformity of the color gradient – from around 52 (blue) to 97 (red) across the diagonal – is further proof of the reliability

of the model for the whole spectrum of yields. Consequently, the model shows an excellent fit and is considered highly reliable for optimizing the transesterification process.

Discussion of key findings

The present results align with [65,66] which highlighted the importance of optimizing catalyst concentration and temperature to maximize biodiesel yield. Predicted results from the quadratic response surface model have been empirically verified and are therefore useful as an optimization tool for producing biodiesel from the seed oil of *V. encelioides.* The results show that high fatty acid methyl ester (FAME) yield can be achieved without compromising biocompatibility by integrating non-edible feedstock and optimizing process control. Such an approach can potentially reduce resource consumption and relieve operational expenses. As noted in references [67,68], these results contribute to the development of sustainable biofuel technologies by providing a framework for optimizing biofuel processing, supported by experimentally validated data.

a) *FT-IR spectroscopy of biodiesel*

V encelioides seed oil FTIR analysis with peaks of absorption consistent with biodiesel standards shown in Fig. 4. It is notable that the peaks at 1742 cm^{-1} (C=O stretching) and 1171 cm^{-1} (C—O stretching) confirm the presence of ester formation. Extra peaks at 2922 cm^{-1} (C–H stretching) and 1457 cm^{-1} (C–H bending) are also associated with the formation of long-chain hydrocarbons, and the absence of an O–H peak around 3300 cm^{-1} suggests little impurity. The high quality of the biodiesel is demonstrated in these findings, as the conversion of triglycerides to fatty acid methyl esters was accomplished efficiently. The FTIR profile of this biodiesel correlates with that of other biodiesels, such as Helianthus annuus and Carthamus tinctorius, which also exhibit ester peaks in 1740–1750 cm^{-1} and 1170–1180 cm^{-1}. However, as they have higher free fatty acid (FFA) levels, these feedstocks require further processing steps [69]. Likewise, as reported by [70], the two-step transesterification process is necessary for Xanthium strumarium with FFA levels above 3 %, and for Tithonia diversifolia, as discussed by [71] with moderate FFA levels. Conversely, its low FFA content (0.16 wt%) enables V. encelioides to achieve better transesterification efficiency and largely reduce the complexity of processing and biodiesel production. In other feedstocks, such as Argemone mexicana and Parthenium hysterophorus, ester peaks are also observed, although with higher FFA content, which therefore requires acid catalysis or a two-step process. Results from the overall FTIR profile also support that V. encelioides is a highly suitable feedstock for biodiesel production among other members of the Asteraceae family.

b) *GC–MS of synthesized biodiesel*

Analysis of biodiesel produced from *V. encelioides* using GC–MS is presented in Table S7. Confirm the ability of triglycerides to convert to FAMEs and give high-quality biodiesel. The chromatogram is shown in Fig. S4. reveals both saturated FAMEs (e.g., Octanoic Acid [C8: Decanoic Acid [C10:0]) and unsaturated FAMEs (Oleic Acid [C18:1], Linoleic Acid [C18:2] with their beneficial properties on cetane number, oxidation stability, cold flow performance, energy density, and combustion efficiency, and enhancing biodiesel properties. These findings correlate with previous studies on other *Asteraceae* families and other biodiesel feedstocks, as well as in the studies of [72], where oleic and linoleic acids, as unsaturated FAMEs, offer their fluidity and oxidative stability. Biodiesels from *Jatropha curcas* and *Pongamia pinnata* reported [73] also indicate the need for the above FAMEs for a balanced cetane number and cold-flow properties. The comparative analysis of biodiesel from various sources further supports similar FAME compositions and confirms their effects on biodiesel quality [74]. *V. encelioides showed* potential as a sustainable and efficient feedstock for high-quality biodiesel.

c) Nuclear magnetic resonance (NMR) spectroscopy of biodiesel

1. The 1HNMR spectroscopy

The biodiesel from *V. encelioides,* as determined by 1H NMR analysis (Fig. S4), confirms efficient conversion via transesterification. The key signals at 0.88–0.89 ppm (terminal methyl groups) and 1.2–1.6 ppm (beta methylene protons) correlate with those of biodiesel derived from other *Asteraceae* members, namely *Helianthus annuus* and *Carthamus tinctorius.* Further evidence that the esterification process occurred is given by the appearance of peaks at 2.0–2.29 ppm (allylic hydrogens) and 4.11–4.33 ppm (ester methylene protons). Formation of the methyl esters was confirmed by the evaporation of the glycerol backbone

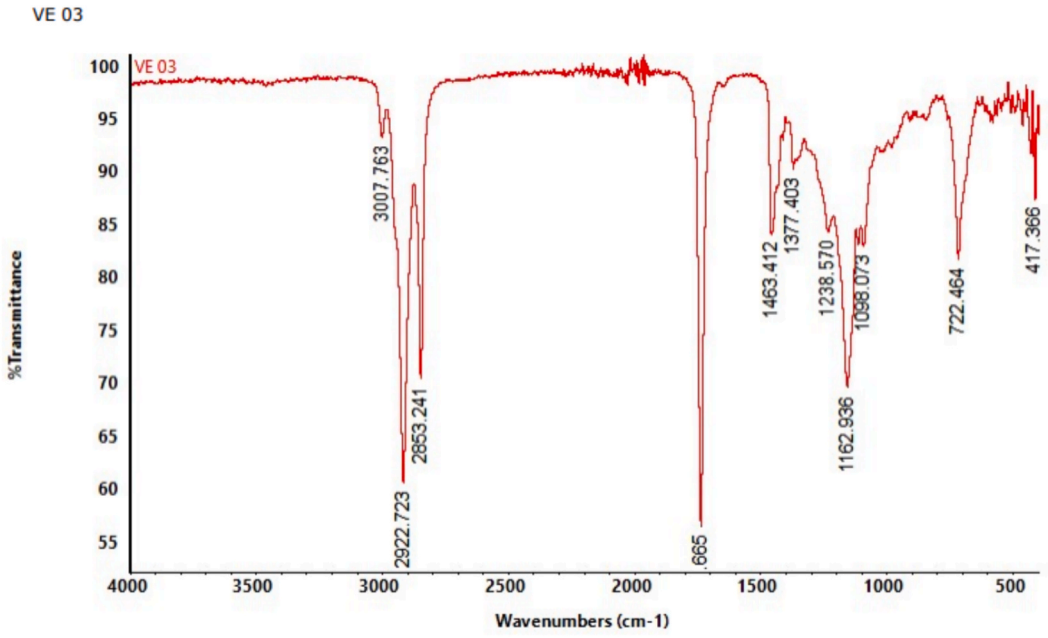

Fig. 4. FT-IR Spectroscopy of VEBD.

indication at ~ 4.2 ppm, and the existence of a singlet at 3.6 ppm (methoxy protons) verifies complete ester conversion. The olefinic hydrogen (5.2–5.38 ppm) identifies an unaltered unsaturated fatty acid chain in biodiesel of *Tithonia diversifolia* and *Xanthium strumarium* [75,76] resulting in improved cold-flow properties. The sole peak at 7.282 ppm is likely due to aromatic protons, possibly from residual solvents or a trace of aromatic compounds. The 1H NMR results are consistent with successful triglyceride esterification to high-purity biodiesel, with preserved unsaturated FAMEs, indicating that *V. encelioides is* a sustainable and efficient feedstock for biodiesel production.

2. The 13CNMR spectroscopy

The 13C NMR analysis of *V. encelioides* is shown in Fig. S6. Biodiesel confirms the transformation of triglycerides to FAMEs. Ester and hydrocarbon structures are reflected in key chemical shifts: terminal methyl groups (22.69 ppm), methylene groups (24.85–27.18 ppm), and bulk methylene signals (29.11–29.76 ppm) showing long saturated hydrocarbon chains characteristic of high-quality biodiesel. Methoxy carbons (–OCH_3) were detected as a distinct signal at 51.39 ppm, confirming that the methyl esters had been formed. Retention of unsaturation is indicated by the presence of aromatic or unsaturated carbons (127.00– 130.86 ppm), and the carbonyl carbons (172.78–173.19 ppm) indicate esterification of triglycerides. This is consistent with biodiesel from other *Asteraceae* members, such as *Tithonia diversifolia* and *Xanthium strumarium* [77],], which also contain unsaturated fatty acid chains that help improve cold flow properties. *V. encelioides* falls in the lower ppm range (22–34 ppm), suggesting greater energy density and enhanced viscosity, rendering it a competitive feedstock for biodiesel production with better chemical stability, oxidative performance, and combustion efficiency as compared to other members of the family *Asteraceae*.

Characterization of V. encelioides seed oil

a) *FT-IR of V. encelioides seed oil*

The FTIR spectrum analysis is shown in Fig. 5.. The *V. encelioides* seed oil supports its suitability as a source material for biodiesel production. There is a peak at 3007 cm^{-1} corresponding to unsaturated fatty acids found usually in oils from the *Asteraceae* family, like *Helianthus annuus* and *Calendula officinalis* oil. At 2923 cm^{-1} and 2853 cm^{-1} peaks correspond to C H stretching of aliphatic chains, which indicate the presence of long hydrocarbon chains important in biodiesel. A substantial peak was observed at 1745 cm^{-1}, further supporting the notion that triglycerides are important precursors for biodiesel production, as reported in *Carthamus tinctorius.* The ester functionalities observed at 1237 cm–1 and 1160 cm–1 indicate that transesterification is possible. The presence of long-chain hydrocarbons confirms, following a peak at 722 cm^{-1} related to CH_2 rocking, a feature common to oil from other *Asteraceae* members and *Xanthium sibricum* [78]. The FTIR analysis reveals that *V. encelioides* seed oil has a composition consistent with other *Asteraceae* oils, making it a feedstock of choice for biodiesel and other biodiesel applications.

Catalyst reusability

The investigation is performed on the various reusability of cobalt chloride as a catalyst for the production of biodiesel under certain reaction conditions: oil to methanol molar ratio of 1:3, the concentration of a catalyst of 0.4 wt% of the total amount of a raw material, the reaction temperature of 60°C, and a reaction time of 120 min. Results indicate that biodiesel yield was high during the first three reuse cycles, with yields of 97 %, 97 %, and 96.5 %, indicating that cobalt chloride is an efficient catalyst under the given reaction conditions. However, 90 % of the yields were observed after the third cycle, and they declined to 90 % for the fourth and fifth cycles. This deactivation is possibly caused by leaching of active cobalt ions during the separation process, by structural changes in the catalyst that decrease its active surface area, or by fouling or deposition of byproducts onto the catalyst surface. Such factors are consistent with previous research in this regard, where metal-based catalysts showed high initial activity but deactivated in subsequent use cycles. These results show that cobalt chloride is an effective catalyst (Fig. S7).

The temperature and time were constant reaction parameters, indicating that changes in biodiesel yield were directly related to catalyst activity. Cobalt chloride exhibited a yield trend as high as achievable under the stated conditions in the first three cycles, making it a suitable candidate for biodiesel production. In addition, this activity declines after three cycles, which makes a reason for future optimization. Studies have shown that supported cobalt catalysts exhibit greater durability and reusability, owing to their greater resistance to structural changes and leaching. In addition, visualizing how higher long-term efficiency could be achieved by further research into alternative metal-based catalysts and bi-metallic catalyst systems [79]. Therefore, cobalt chloride demonstrated excellent catalytic efficiency for biodiesel production through the third cycle, with yields exceeding 96 %. It highlights the need to understand catalyst deactivation mechanisms to introduce a

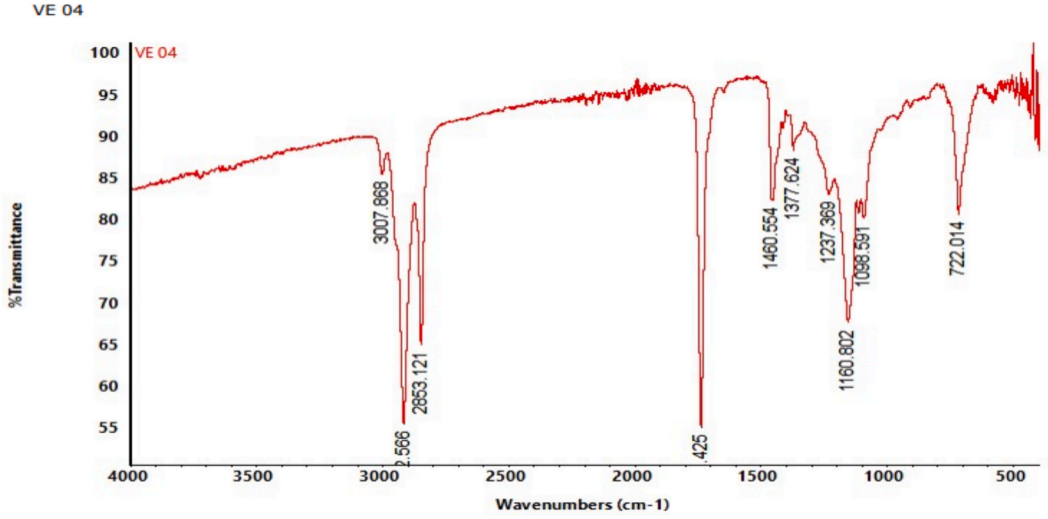

Fig. 5. FT-IR of *V. encelioides* seed oil.

fourth cycle and achieve higher yields. These findings provide important additions for sustainable biodiesel production and the use of metal-based catalysts.

Techno-economic analysis of *Verbesina encelioides* biodiesel production

Although *V. encelioides* seeds are low-cost, the oil extraction, purification, and characterization techniques (e.g., GC, FTIR, NMR) entail high operational costs, which significantly contribute to overall production expenses. Feedstock collection is inexpensive (~10 % of total cost), whilst processing and analytical characterization account for ~ 60–65 %, with catalyst, methanol, energy, and labor making up the remaining 25–30 % as shown in Table S8.

Uncertainty analysis of *Verbesina encelioides* biodiesel

The line graph (Fig. S8) shows the effect of reaction temperature on the biodiesel yield from *V. encelioides*. Error bars represent experimental error (the experimental uncertainty, or the standard deviation). Each bar represents the average yield from three replicates conducted at different temperatures. The data show a general trend of increasing biodiesel yield with increasing temperature, reaching an optimum, and then a slight decrease (suggesting that this could be due to methanol volatilization or catalyst deactivation at higher temperatures). The error bars are relatively small, indicating robust reproducibility and little experimental variability. Overall, the graph shows that temperature has a considerable effect on the efficiency of the transesterification process, and the uncertainties presented improve the reliability and clarity of the results in Table S9.

Conclusion

This investigation examines the potential of *Verbesina encelioides* seed oil as a suitable feedstock for biodiesel production via a novel method using cobalt oxide as a nanocatalyst. The efficiency and sustainability aspects of this methodology are highlighted in the study, as are its contributions to the broader discussion of renewable energy sources. The isolated seed oil showed a high extraction yield of 33 wt% and a low free fatty acid content of 0.16 wt%. These characteristics enabled a simplified one-step transesterification process, with a corresponding decrease in operational complexity and an increase in overall process efficiency. The cobalt oxide nanocatalyst developed from the seed husk of V. encelioides exhibited greater surface area, porosity, and structural stability than conventional catalysts. Consequently, the biocatalyst achieved a 97 % yield in biodiesel production and demonstrated greater catalytic activity than conventional industrial catalysts, demonstrating its efficiency in the biodiesel synthesis process. The resulting biodiesel had physicochemical properties like those of regular diesel fuel, characterized by a high concentration of oleic acid methyl ester, which improved the oxidative stability, cold flow properties, and combustion efficiency of the fuel. In addition, reusability studies showed that the catalyst maintained a high level of activity over several reaction cycles, suggesting its use as an economically and environmentally feasible method for producing biodiesel.

Future work scope

Future investigations should focus on reaction optimization and catalyst recycling to improve process efficiency and durability. Engine performance and emissions must be validated to demonstrate real-world applicability. These results lay a solid foundation for evaluating the sustainability of *V. encelioides-derived* biodiesel, given its potential to meet renewable energy goals and to control invasive weeds.

CRediT authorship contribution statement

Farzana: . **Fahd A. Nasr:** Writing – review & editing, Resources, Data curation. **Mushtaq Ahmad:** Writing – review & editing, Supervision, Software, Conceptualization. **Mohammed Al-zharani:** Writing – review & editing, Supervision, Software, Methodology. **You-Cai Xiong:** Writing – review & editing, Validation, Project administration, Investigation. **Lina M. Alneghery:** Writing – review & editing, Resources, Funding acquisition. **Hong-Yan Tao:** Writing – review & editing, Visualization, Data curation. **Najeeb Ullah:** Writing – review & editing, Writing – original draft, Investigation. **Ahmad Mustafa:** Writing – review & editing, Writing – original draft, Conceptualization. **Shazia Sultana:** Writing – review & editing, Visualization, Validation, Supervision.

Declaration of competing interest

The authors declare that they have no known competing financial interests or personal relationships that could have appeared to influence the work reported in this paper.

Acknowledgments

This work was supported and funded by the Deanship of Scientific Research at Imam Mohammad Ibn Saud Islamic University (IMSIU) (grant number IMSIU-DDRSP2501).

Appendix A. Supplementary data

Supplementary data to this article can be found online at https://doi.org/10.1016/j.seta.2025.104785.

Data availability

Data will be made available on request.

References

[1] Clack CT, et al. *Evaluation of a proposal for reliable low-cost grid power with 100% wind, water, and solar*. Proc Natl Acad Sci 2017;114(26):6722–7.
[2] Holechek JL, et al. *A global assessment: can renewable energy replace fossil fuels by 2050?* Sustainability 2022;14(8):4792.
[3] Abban OJ, et al. *Renewable energy, economic growth, and CO2 emissions contained Co-movement in African oil-producing countries: a wavelet based analysis*. Energ Strat Rev 2022;44:100977.
[4] Lark TJ, et al. *Environmental outcomes of the US renewable fuel standard*. Proc Natl Acad Sci 2022;119(9):e2101084119.
[5] Zhang S, et al. *Global readiness for carbon neutrality: from targets to action*. Environ Sci Ecotechnol 2025;25:100546.
[6] Elishav O, et al. *Progress and prospective of nitrogen-based alternative fuels*. Chem Rev 2020;120(12):5352–436.
[7] Hill J, et al. *Environmental, economic, and energetic costs and benefits of biodiesel and ethanol biofuels*. Proc Natl Acad Sci 2006;103(30):11206–10.
[8] Rouhany M, Montgomery H. *Global biodiesel production: the state of the art and impact on climate change*. Biodiesel: from production to combustion 2018:1–14.
[9] Mahlia T, et al. *Patent landscape review on biodiesel production: technology updates*. Renew Sustain Energy Rev 2020;118:109526.
[10] Singh D, et al. *A review on feedstocks, production processes, and yield for different generations of biodiesel*. Fuel 2020;262:116553.
[11] Alagha SM, Salih R. *Review the studies of mass transfer and kinetic modeling for production the biodiesel by the transesterification method and the impact of some selected factors. IOP Conference Series: Earth and Environmental Science*. IOP Publishing; 2023.
[12] Islam S, et al. *Advancement in utilization of nanomaterials as efficient and recyclable solid catalyst for biodiesel synthesis*. Cleaner Chem Eng 2022;3:100043.
[13] Panahi A, et al. *Green auto-combustion synthesis and characterization of TmVO4 nanostructures in the presence carbohydrate sugars and their application as visible-light photocatalyst*. Sol Energy 2023;258:372–82.
[14] Khatami M, Iravani S. *Green and eco-friendly synthesis of nanophotocatalysts: an overview*. Comments Inorg Chem 2021;41(3):133–87.
[15] Faraji AR, Mosazadeh S, Ashouri F. *Synthesis and characterization of cobalt-supported catalysts on modified magnetic nanoparticle: green and highly efficient heterogeneous nanocatalyst for selective oxidation of ethylbenzene, cyclohexene and oximes with molecular oxygen*. J Colloid Interface Sci 2017;506:10–26.

[16] Khafaga DS, et al. *Green nanobiocatalysts: enhancing enzyme immobilization for industrial and biomedical applications*. PeerJ 2024;12:e17589.
[17] Thompson PB. *The agricultural ethics of biofuels: the food vs. fuel debate*. Agriculture 2012;2(4):339–58.
[18] Zihare, L., R. Soloha, and D. Blumberga, *The potential use of invasive plant species as solid biofuel by using binders.* 2018.
[19] Alkotami L, et al. *Targeted engineering of camelina and pennycress seeds for ultrahigh accumulation of acetyl-TAG*. Proc Natl Acad Sci 2024;121(47):e2412542121.
[20] Akleshwar Mathur, A.M. and M. Sherwani, *Verbesina encelioides seed oil: a new rich source of vernolic acid.* 2006.
[21] Mehal K. *Verbesina encelioides: a fast spreading weed in semi-arid regions of North-Western India. is climate change responsible?* J Sci Res 2021;13(1):275–82.
[22] Santos KA, da Silva EA, da Silva C. *Ultrasound-assisted extraction of favela (Cnidoscolus quercifolius) seed oil using ethanol as a solvent*. J Food Process Preserv 2021;45(6):e15497.
[23] Dutta R, et al. *Experimental investigation of fracturing-fluid migration caused by spontaneous imbibition in fractured low-permeability sands*. SPE Reserv Eval Eng 2014;17(01):74–81.
[24] Arshad S, et al. *Assessing the potential of green CdO2 nano-catalyst for the synthesis of biodiesel using non-edible seed oil of Malabar Ebony*. Fuel 2023;333:126492.
[25] Vovk H, et al. *Enzymatic pretreatment of plant cells for oil extraction*. Food Technol Biotechnol 2023;61(2):160–78.
[26] Haryono, I., et al., *Cold start ability test for diesel passenger cars using thirty percent palm biodiesel and precipitation in low temperature ambient.* 2023.
[27] Ahmad R, et al. *Synthesis, molecular structure and urease inhibitory activity of novel bis-Schiff bases of benzyl phenyl ketone: a combined theoretical and experimental approach*. Saudi Pharmaceutical Journal 2023;31(8):101688.
[28] Dong Y, et al. *The road of lipid migration in flaxseed (Linum usitatissimum L.) during germination*. Food Res Int 2025;201:115581.
[29] Alsaiari M, et al. *Efficient application of newly synthesized green Bi2O3 nanoparticles for sustainable biodiesel production via membrane reactor*. Chemosphere 2023;310:136838.
[30] Xu W, et al. *Quantifying atmospheric nitrogen deposition through a nationwide monitoring network across China*. Atmos Chem Phys 2015;15(21):12345–60.
[31] Baskar G, Soumiya S. *Production of biodiesel from castor oil using iron (II) doped zinc oxide nanocatalyst*. Renew Energy 2016;98:101–7.
[32] Hazmi B, et al. *Synthesis and characterization of bifunctional magnetic nano-catalyst from rice husk for production of biodiesel*. Environ Technol Innovation 2021;21:101296.
[33] Salmalian S, Mahmoodi NO, Sheykhan M. *One-pot multicomponent synthesis of novel chromene derivatives using new organic phosphate salt catalysts*. ChemistrySelect 2023;8(33):e202204635.
[34] Nisa B, et al. *Biodiesel production using wild apricot (Prunus aitchisonii) seed oil via heterogeneous catalysts*. Molecules 2022;27(15):4752.
[35] Rozina, et al. *Biodiesel synthesis and physiochemical analysis of Taraxacum officinale FH Wigg seed oil*. Int J Environ Sci Technol 2019;16(8):4103–12.
[36] Semyonova, A., et al., *Transesterification of Rapeseed Oil to Biodiesel Using a Nanomembrane-Based Reactor*. Available at SSRN 4562164.
[37] Akhtar MN, et al. *Tunable and wideband high-performance rare earth-doped Ni-Mg-Cu-Zn nano ferrite-based meta-absorbers for C-band application*. J Rare Earths 2025;43(1):124–32.
[38] Bousba D, et al. *Efficient biodiesel production from recycled cooking oil using a NaOH/CoFe2O4 magnetic nano-catalyst: synthesis, characterization, and process enhancement for sustainability*. Energ Conver Manage 2024;300:118021.
[39] Mondal A, et al. *Cobalt nanoparticles as reusable catalysts for reduction of 4-nitrophenol under mild conditions*. Bull Mater Sci 2017;40(2):321–8.
[40] Ezzat SM, et al. *Antiprotozoal activity of major constituents from the bioactive fraction of Verbesina encelioides*. Nat Prod Res 2017;31(6):676–80.
[41] Jian J, et al. *Constraining estimates of global soil respiration by quantifying sources of variability*. Glob Chang Biol 2018;24(9):4143–59.
[42] Malik G, et al. *Genomics, physiology and molecular breeding approaches for improving crop productivity under salt stress: progress and prospects*. Salt Stress Responses Plants 2017;179:405–34.
[43] Wang J, et al. *Cobalt nanoparticles encapsulated in nitrogen-doped carbon as a bifunctional catalyst for water electrolysis*. J Mater Chem A 2014;2(47):20067–74.
[44] Yang K, et al. *Unveiling the reaction mechanism of nitrate reduction to ammonia over cobalt-based electrocatalysts*. J Am Chem Soc 2024;146(19):12976–83.
[45] Chattopadhyay S, et al. *Surface-modified cobalt oxide nanoparticles: new opportunities for anti-cancer drug development*. Cancer Nanotechnol 2012;3(1):13–23.
[46] Mehrafza M, et al. *Green fabrication of cobalt oxide nanoparticles by bacillus megaterium and their antibacterial activities*. BioNanoScience 2024;14(3):2315–26.
[47] Bukhamsin HA, et al. *Catalytic reductive degradation of 4-nitrophenol and methyl orange by novel cobalt oxide nanocomposites*. Catalysts 2024;14(1):89.
[48] Zahid MU, et al. *A comparative study of PEGylated cobalt oxide nanoparticles (Co3O4-NPs) and cobalt sulfide nanoparticles (Co9S8-NPs) for biological and photocatalytic applications*. BioNanoScience 2024;14(2):643–60.
[49] Soni A, et al. *Fe-doped nano-cobalt oxide green catalysts for sulfoxidation and photo degradation*. Clean Techn Environ Policy 2024;26(11):3869–80.
[50] Saranya V, et al. *Unravelling the catalytic activity of copper cobalt oxide-nickel cobalt oxide composites for efficient counter electrode performance in DSSCs*. J Alloy Compd 2024;988:173993.
[51] Monshi A, Foroughi MR, Monshi MR. *Modified Scherrer equation to estimate more accurately nano-crystallite size using XRD*. World J Nano Sci Eng 2012;2(3):154–60.
[52] Mohiddin MNB, et al. *Waste oil to biodiesel*. In: *Advanced Technology for the Conversion of Waste into Fuels and Chemicals*. Elsevier; 2021. p. 337–55.
[53] Emmanuel O, et al. *Valorization of waste seed oil from Cupressus macrocarpa L. for biodiesel production via green-synthesized iron oxide nanoparticles: a sustainable approach toward decarbonization*. Next Energy 2025;7:100218.
[54] Meky AI, et al. *Hydrothermal fabrication, characterization and RSM optimization of cobalt-doped zinc oxide nanoparticles for antibiotic photodegradation under visible light*. Sci Rep 2024;14(1):2016.
[55] Cardoso C, et al. *Optimizing phosphorus recovery from an acidic pulp stream with cobalt ferrite nanoparticles: a methodology for pulp mills*. Colloids and Surfaces C: Environmental Aspects; 2025.
[56] Ibrahim M, et al. *Waste cooking oil processing over cobalt aluminate nanoparticles for liquid biofuel hydrocarbons production*. Sci Rep 2023;13(1):3876.
[57] Qi Q, et al. *Enhancement of methanogenic performance by gasification biochar on anaerobic digestion*. Bioresour Technol 2021;330:124993.
[58] Dairo O, et al. *INFLUENCE OF CATALYST QUANTITY AND REACTION TIME ON IN-SITU PRODUCTION OF BIODIESEL FROM RAW CASTOR BEAN SEED USING RESPONSE SURFACE METHODOLOGY*. Journal of Natural Sciences. Eng Technol 2011;10(2):146–57.
[59] Ghadge SV, Raheman H. *Process optimization for biodiesel production from mahua (Madhuca indica) oil using response surface methodology*. Bioresour Technol 2006;97(3):379–84.
[60] Lee AF, et al. *Heterogeneous catalysis for sustainable biodiesel production via esterification and transesterification*. Chem Soc Rev 2014;43(22):7887–916.
[61] Karpagam R, et al. *Green energy from Coelastrella sp. M-60: Bio-nanoparticles mediated whole biomass transesterification for biodiesel production*. Fuel 2020;279:118490.
[62] Hamze H, Akia M, Yazdani F. *Optimization of biodiesel production from the waste cooking oil using response surface methodology*. Process Saf Environ Prot 2015;94:1–10.
[63] Elgharbawy AS, et al. *A review on biodiesel feedstocks and production technologies*. J Chil Chem Soc 2021;66(1):5098–109.
[64] Bahadoran A, et al. *Biodiesel production from waste cooking oil using heterogeneous nanocatalyst-based magnetic polyaniline decorated with cobalt oxide*. Fuel 2022;319:123858.
[65] Razzaq L, et al. *Maximising yield and engine efficiency using optimised waste cooking oil biodiesel*. Energies 2020;13(22):5941.
[66] Zhang W, et al. *Efficient and economic transesterification of waste cooking soybean oil to biodiesel catalyzed by outer surface of ZSM-22 supported different Mo catalyst*. Biomass Bioenergy 2022;167:106646.
[67] Tan D, et al. *Evaluation and optimization of hydrogen addition on the performance and emission for biodiesel dual-fuel engines with different blend ratios based on the response surface method*. Energy 2023;283:129168.
[68] Liang X, et al. *Application of response surface methodology for the joint optimization of performance and emission characteristics of a diesel engine*. Int J Green Energy 2021;18(7):697–707.
[69] Phukan K, Chutia GP, Chutia S. *Synthesis of biodiesel from Indigenous Xanthium Strumarium (Cocklebur) Non-Edible Oil Available in Assam, India*. ChemistrySelect 2022;7(27):e202201342.
[70] Pawar, S., et al., *Studies on Xanthium strumarium L. seed oil: biodiesel synthesis and process optimization.* Materials Today: Proceedings, 2022. **66**: p. 2169-2177.
[71] Farouk SM, et al. *Recent advances in transesterification for sustainable biodiesel production, challenges, and prospects: a comprehensive review*. Environ Sci Pollut Res 2024;31(9):12722–47.
[72] Verma S, Sahu D, Almutairi BO. *Production and characterization of biodiesel fuel produced from third-generation feedstock*. Front Mater 2024;11:1454120.
[73] Esipovich AL, et al. *A comprehensive study on physicochemical properties of fatty acid esters derived from different vegetable oils and alcohols and their potential application*. Energies 2024;17(24):6407.
[74] Nisar S, et al. *Trends in widely used catalysts for fatty acid methyl esters (Fame) production: a review*. Catalysts 2021;11(9):1085.
[75] Kaur M, et al. *Isolation and characterization of constituents from the leaves of xanthium strumarium and their evaluation for antioxidant and antimicrobial potential*. Nat Prod Chem Res 2015;3(2):1000168.
[76] Jan HA, et al. *Aleurites moluccana as a potential non-edible feedstock for industrial-scale biodiesel synthesis using homemade zinc oxide nanoparticles as a catalyst*. Waste Biomass Valoriz 2024;15(2):1081–95.
[77] Naureen R, et al. *Synthesis, spectroscopic and chromatographic studies of sunflower oil biodiesel using optimized base catalyzed methanolysis*. Saudi J Biolo Sci 2015;22(3):332–9.
[78] Alihellal D, Chibane L, Slimani M-E-A. *Modeling and simulation of the deactivation by sintering of the cobalt catalyst during the fischer-tropsch reaction*. J Mech Eng Res 2019;2(1).
[79] Khan I, Han L, Khan H. *Renewable energy consumption and local environmental effects for economic growth and carbon emission: evidence from global income countries*. Environ Sci Pollut Res 2022;29(9):13071–88.